Journal of Lake and Reservoir Management 14(2-3):238-253, 1998

The Optical Water Quality of Cannonsville Reservoir: Spatial and Temporal Patterns, and the Relative Roles of Phytoplankton and Inorganic Tripton[1]

S.W. Effler and M.G. Perkins
Upstate Freshwater Institute
P.O. Box 506, Syracuse, NY 13214

D.L. Johnson
Environmental Chemistry
SUNY College of Environmental Science and Forestry
1 Forestry Drive, Syracuse, NY 13210

ABSTRACT

Effler, S. W., M. G. Perkins and D. L. Johnson. 1998. The optics of Cannonsville Reservoir: Spatial and temporal structures, and the relative roles of phytoplankton and inorganic tripton. Lake and Reserv. Manage. 14(2-3):238-253.

Longitudinal and temporal distributions of optical properties, and the relative role of selected light attenuating constituents in regulating light penetration, in Cannonsville Reservoir, NY, in 1995 are documented. The analysis is supported by field measurements of light penetration; the angular distribution of irradiance (reflectance); and the spectral quality of penetrating light; laboratory measurements of turbidity, chlorophyll, gelbstoff, and microscopy-based individual particle size and elemental chemistry; and calculations of absorption and scattering coefficients and their components. Longitudinal gradients in attenuating components, and therefore optical properties, prevailed along the main axis of the reservoir; light attenuation and the relative role of scattering decreased with the approach to the dam. Large temporal variations in optical characteristics occurred. These dynamics were mostly controlled by variations in phytoplankton biomass in spring and early summer, when the reservoir was full, but resuspended inorganic tripton (non-phytoplankton particles; suspensoids) became the regulating component as the reservoir was drawn down. Quantitative optical frameworks (models) are applied to simulate light penetration conditions that would have prevailed for scenarios of reductions in phytoplankton biomass and/or inorganic tripton.

Key Words: reservoir, optics, phytoplankton, inorganic tripton, inorganic suspensoids, Secchi disc, clarity, light attenuation, light absorption, light scattering.

The behavior of light in water has important water quality implications, because it regulates visual esthetics and (along with nutrients and temperature) phytoplankton growth. The extent of light penetration within a given water body is an area of concern to lake and water supply managers. For example, certain minimum Secchi disc transparency (SD, m) values (a measure of clarity) are required in a number of states to support swimming. Improvements in clarity are often a primary motivation for restoration of culturally eutrophic lakes (Cooke et al. 1993). Water supplies are required to provide water with turbidity values (T_n, NTU; measured with a nephelometric turbidimeter) below a specified standard. It is important that managers recognize that T_n is an optical measurement (Kirk 1994), distinctly different from the concentration of suspended solids (TSS). The same TSS value can be associated with a rather wide range of T_n values, depending primarily on particle size distribution (Kirk 1985, 1994). Unfortunately, the term clarity has been used interchangeably by limnologists and water suppliers in reference to SD and T_n. These two measurements differ fundamentally in their response to attenuating processes, and they cannot be uniquely specified by each other (Effler 1988).

The extent of light penetration is regulated by two

[1] Contribution No. 167 of the Upstate Freshwater Institute.

attenuating processes: absorption and scattering. The intensities of these processes are specified by the magnitudes of the absorption (a, m^{-1}) and scattering (b, m^{-1}) coefficients. These coefficients are **inherent** optical properties that are intrinsic features of the medium. They are not easily subject to direct determination but they can be estimated from measured (**apparent**) optical properties (Kirk 1981b). Other **inherent** properties are the beam attenuation coefficient ($c = a + b$, m^{-1}) and the angular scattering function (which tends to be rather uniform for lakes and reservoirs) (Kirk 1994). The magnitudes of a and b are regulated by the composition and concentration of the various attenuating materials. Absorption has been partitioned into four components by Kirk (1994): water itself, dissolved yellow substances (gelbstoff), phytoplankton, and tripton (non-phytoplankton particles). The spectral character of these absorbing materials differs substantially (Kirk 1994, Weidemann and Bannister 1986) over the photosynthetically active radiation (PAR) wavelength interval (400 to 700 nm), and the spectral quality of light changes as it penetrates the water column as a result of absorption by these constituents. Scattering, associated almost entirely with particles, increases attenuation by causing increases in the pathlength that photons must traverse (e.g., increasing the likelihood of absorption). These particles can have autochthonous (e.g., phytoplankton and certain minerals) or allochthonous (e.g., clays) origins. The value of b has been found to vary little with wavelength in the PAR interval compared to a (Phillips and Kirk 1984).

Wide differences in **apparent** optical properties, such as SD, vertical attenuation coefficients (K_x, m^{-1}), and reflectance (R, dimensionless) occur between lakes, and temporally and spatially within lakes. These are associated with differences in the composition and concentration of light attenuating substances and thus the magnitudes of a and b. Partitioning light attenuation and related apparent optical properties according to the contributions of absorption and scattering, and the materials regulating these processes, is essential in establishing the appropriate foci and realistic goals for management efforts concerned with optical aspects of water quality. For example, if particles of terrigenous origin (i.e., tripton) regulate SD and T_n, a management program that is successful in reducing phytoplankton growth may achieve little in the way of decreasing T_n and increasing SD. In such a case, an alternate management program, such as erosion control in the watershed, may be more effective.

Here we document the spatial gradients and dynamics in apparent optical properties and measures of attenuating components in the upper waters of Cannonsville Reservoir, NY, over the spring-fall interval of 1995. Estimates of a and b, and the contributions of attenuating materials, are presented. Materials and processes regulating the optical properties of the reservoir are delineated based on existing optical theory. These findings are discussed within the context of supporting the development of management strategies to maintain or improve the optical esthetics of this reservoir. The analysis is of particular interest because this impoundment supported relatively high concentrations of both tripton (Effler et al. 1998) and phytoplankton pigments (Effler and Bader 1998) during the study period.

Methods

Study System

Cannonsville Reservoir, NY, is a eutrophic water supply and flow augmentation impoundment for New York City (NYC; ~ 190 km away). The principal axis of the reservoir corresponds to the bed of the West Branch of the Delaware River (WBDR; Fig. 1). Approximately 80% of the inflow to the reservoir is received from WBDR. Cannonsville Reservoir has a crest capacity of 373 x 10^6 m^3, a corresponding surface area of 19.3 x 10^6 m^2, and mean depth of ~ 19 m. The average "completely mixed" flushing rate of the reservoir has been about 2.2 y^{-1} since it started operating in 1966 (Owens et al. 1998b). A major drawdown of the reservoir surface was experienced in 1995 (Owens et al. 1998b).

Detailed descriptions of the reservoir's operation and hydrology (Owens et al. 1998b), limnology (Effler and Bader 1998), and material loading (e.g., suspended solids, nutrients) to the system (Longabucco and Rafferty 1998) have been presented elsewhere in this issue of the journal. Gradients in various water quality

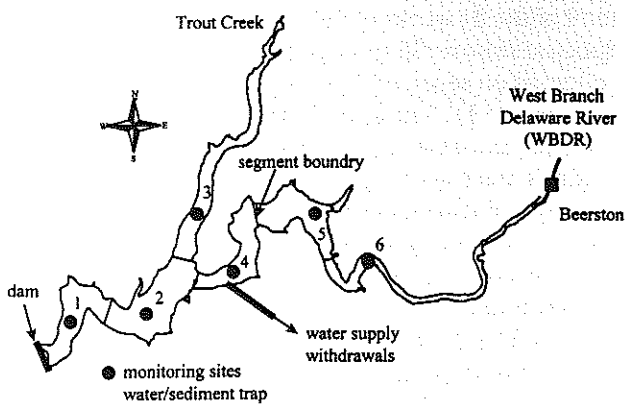

Figure 1.–Cannonsville Reservoir map with sampling sites, and locations of water supply intakes, dam, and Beerston, NY.

parameters, including phytoplankton biomass and other trophic state indicators (Effler and Bader 1998), and concentrations and deposition rates of particulate constituents (Effler and Brooks 1998), prevail from the upstream boundary (Beerston, Fig. 1) of the reservoir (e.g., highest concentrations and deposition rates) to the dam (Fig. 1). The operation of the sediment resuspension process in the reservoir over the spring-fall interval of 1995 was documented and coupled to drawdown (Effler et al. 1998). The impact of the resuspended tripton on the impoundment's optical characteristics, including turbidity, receives special attention in the analysis presented here.

Sampling and Measurements

The utility of the various measurements made in this study (Table 1) to characterize the optical regime of the reservoir and support partitioning of the contributions of specific materials and processes has been reviewed elsewhere (Perkins and Effler 1996, Kirk 1994). Optical measurements were made and related sampling conducted between 1000 and 1500 hours (eastern daylight time) at as many as six longitudinal positions on Cannonsville Reservoir (Fig. 1) and as often as weekly over the April-October interval of 1995. These six sites are the same ones adopted for water quality monitoring (Effler and Bader 1998, Effler et al. 1998) and sediment trap collections (Effler and Brooks 1998) for the same period. Optical field measurements made routinely at all sites included Secchi disc transparency (SD, m) and scalar PAR irradiance (E_o) profiles (Table 1). The scalar irradiance (spherical) sensor (LI-COR 193SB) was powered by a Seabird Sealogger Profiler (Model SBE 25). Readings were recorded at a rate of 8 s^{-1}, with an instrument descent rate of about 1.2 $m \cdot s^{-1}$. Downwelling (E_d) and upwelling (E_u) PAR cosine irradiance (flat sensors) profiles were collected at three sites (1, 4 and 5; Fig. 1) for 9 of the 31 weeks of field measurements (Table 1). Spectral downwelling irradiance ($E_{d(\lambda)}$) profiles were collected on seven of these nine occasions at the same sites (Table 1). The size of the system, the number of sites, and the time required for the field measurements made it necessary to collect the cosine sensor and spectroradiometer profiles the day before (SD measured on both days) the routine E_o measurements and sampling were conducted. Irradiance measurements were made to depths below the 10% light level ($z_{0.1}$). The "asymptotic radiance distribution" is generally assumed to be established at $z_{0.1}$ (Kirk 1994, Weidemann and Bannister 1986). The quantum sensors (E_o, E_d, and E_u) measure PAR with nearly ideal quantum response. The relative error (spectral response) of the cosine sensors is < 5%; for the scalar sensor it is <7% (LI-COR 1982).

Laboratory analyses (Table 1) of T_n, chlorophyll (Chl), and gelbstoff ($a_{y(440)}$) were conducted weekly on samples collected from depths of 0 and 3 m, to represent conditions extending from the surface to about the 10% light level. Chlorophyll [here as total chlorophyll, equal to the sum of chlorophyll *a*, *b*, and *c* (Parsons et al. 1984)] is the widely accepted, but imperfect (e.g., Kirk 1994), measure of phytoplankton biomass. Gelbstoff ($a_{y(440)}$) was determined as the absorption of filtered (0.45-μm Microfiltration cellulose acetate) water from absorbance measurements at 440 nm (corrected by absorbance at 700 nm), with a Carey 219 spectrophotometer (10 cm path length). Additionally, complete gelbstoff spectra ($a_{y(\lambda)}$, 400 to 700 nm; Table 1) were determined on the days of E_d, E_u, and $E_{d(\lambda)}$ measurements.

The particle assemblages of samples collected on 7 of the routine sampling days (depth of 3m) were analyzed by scanning electron microscopy equipped with automated image analysis and x-ray energy spectroscopy (SAX). This individual particle analysis (IPA) technique provided both physical (size, shape, count) and chemical (elemental) characterizations of particles >0.5 μm in diameter. An additional six samples (3 m) were morphometrically characterized (scanning electron microscopy with automated image analysis, only). Detailed descriptions of sample preparation and analytical procedures for SAX analyses have been presented by Yin and Johnson (1984) and Johnson et al. (1991). Information for 9 variables was obtained that includes relative x-ray emission intensity for 25 elements (Na and higher atomic number), net x-ray count rate, width, length, and projected feature area. These variables were used to establish a simple classification scheme of six particle types (according to chemistry): organic, calcium-rich, clays, iron-rich, silica, and other (see Effler et al. 1998). Results of these analyses were presented by Effler et al. (1998) in the form of particle class (6) concentrations, % composition, and the particle cross-sectional area per unit volume (PAV; see Johnson et al. 1991).

The PAV data were partitioned to estimate the contribution of inorganic tripton by subtracting components associated with phytoplankton. It was assumed that "organic" features and the diatom fraction of the silica particle class (Table 1 of Effler et al. 1998) were of phytoplankton origin. The automated IPA characterizations of SAX cannot, at present, distinguish between quartz and the siliceous frustules of diatoms. The diatom fraction was estimated based on visual examination (i.e., manual instead of automated) of all 13 IPA samples with the electron microscope. The inorganic tripton PAV for the seven samples with

Table 1.–Protocols for measurement and calculations of optical characteristics of Cannonsville Reservoir, NY.

Protocols	Comments/Equations/References
A. Field	
Secchi disc transparency (SD; m)	20-cm-diameter black and white quadrant disc
broad band (PAR; quantum)	
irradiances ($\mu E \cdot m^{-2} \cdot s^{-1}$)	
scalar (E_o)	LI-COR 193 SB sensor
downwelling (E_d) and upwelling E_u cosine	LI-COR 192 sensors (2)
spectral downwelling irradiance ($E_{d(\lambda)}$; $\mu E \cdot m^{-2} \cdot s^{-1}$)	LI-COR 1880 UW spectroradiometer
transmissometry (c_{660}; m^{-1})	at 660 nm; Chelsea Instrument
B. Laboratory	
total chlorophyll (Chl; $mg \cdot m^{-3}$)	Parsons et al. (1984)
turbidity (T_n; NTU)	APHA (1992); HACH 2100 turbidimeter
gelbstoff ($a_{y(\lambda)}$; m^{-1})	Davies-Colley and Vant (1987)
IPA (PAV)	Johnson et al. 1991
Calculations	
vertical attenuation coefficients	$K_{x(z)} = -\frac{d\ln E_{x(x)}}{dz}$ (1)
scalar irradiance (K_o; m^{-1})	$K_{x(z)}$ - attenuation coefficient at depth z, and irradiance type x
downwelling (K_d; m^{-1})	
upwelling (K_u; m^{-1})	$E_{x(z)}$ - irradiance type x, at depth z
net downwelling ($\bar{\mu} \cdot K_E$; m^{-1})	
spectral downwelling ($K_{d(\lambda)}$; m^{-1})	2-nm wavelength intervals
integrated spectral for PAR ($K_{d(PAR)}$; m^{-1})	Jerome et al. (1983)
reflectance (R; dimensionless)	$R = \frac{E_u}{E_d}$ (2)
absorption coefficient (a; m^{-1})	$a = \bar{\mu} . KE$ (3) $\bar{\mu}$ - average cosine, from R at $z_{0.1}$ and relationship of Kirk (1981b)
scattering coefficient (b; m^{-1})	$b = a \cdot (b/a)$ (4) ratio b/a from R at $z_{0.1}$, and relationship of Kirk (1981b)
spectral average absorption	
coefficient (a_x) for water (a_w; m^{-1}) and gelbstoff (a_y; m^{-1})	$a_x =$ (5)
	$a_{w(\lambda)}$ - from Smith and Baker (1981)
spectral average absorption coefficient for particles (a_p; m^{-1})	$a_p = a - (a_w + a_y)$ (6)

chemical characterization was calculated (as a residual) by subtraction of "diatom PAV" and "organic PAV" from the total PAV. For the six samples without chemical characterization, the tripton PAV was calculated based on the average "diatom PAV" and "organic PAV" values. Uncertainties in these calculations are dominated by the "diatom PAV" assessment, as the silica only subclass (i.e., quartz plus diatoms) PAV averaged 20.5% (n=7, range 9 to 35.2%) of the total, while "organic PAV" averaged only 2.3% (n=7, range 0.8 to 6.4%). It is unlikely that the error in the calculation procedure adopted here exceeded one-half of the summation of the maxima of the silica only subclass and "organic" PAV values (i.e., ≤ 21% relative error).

Calculations

Vertical attenuation coefficients were calculated according to Beer's Law, at depths bounding $z_{0.1}$ [Eq. (1), Table 1]. A scalar sensor supports the determination of K_o (m^{-1}). A single cosine sensor, facing upward, supports the determination of K_d (m^{-1}, Table 1). A two cosine sensor configuration, one facing upward, the other facing downward, at the same depth, supports additionally the determination of reflectance [R, Eq. (2), Table 1; a measure of the angular distribution of underwater irradiance], K_E (m^{-1}), and K_u (m^{-1}, Table 1). These vertical attenuation coefficients for PAR have been observed to be nearly equivalent (Kirk 1994, Weidemann and Bannister 1986). Attenuation coefficients for spectral downwelling irradiance ($K_{d(\lambda)}$) were calculated at 2-nm intervals (Table 1) and integrated for the PAR interval for comparison to attenuation coefficients determined from quantum (PAR) sensors.

The spectral average values of a and b for PAR were estimated according to the protocol set forth by Kirk (1981b) and adopted in subsequent studies of many different systems (Kirk 1994). Kirk's (1981b) functions were used to obtain the average cosine (another measure of the angular distribution of irradiance) and the ratio b/a from the measured R. The value of a at $z_{0.1}$ was calculated according to the Gershun-Jerlov equation [Eq. (3), Table 1]. The value of b is then calculated from a and the ratio of b/a [Eq. (4), Table 1].

Errors in K_d and R at $z_{0.1}$ will propagate to the estimates of a [Eq. (3)] and b [Eq. (4)] (Weidemann and Bannister 1986). The error in calibration between detectors (E_d and E_u) is expected to be less than 5% (LI-COR 1982). Additional errors in K_d were undoubtedly introduced on non-clear sky days due to unavoidable changes in incident irradiance during the collection of profiles. We expect these to be usually <5%, based on replicate profiles collected on other systems under a range of incident light conditions. We interpolated the $\bar{\mu}$ as a function of R relationships for the different zenith angles, presented by Kirk (1981b), to reduce potential seasonal errors (≤ 10%) (Weidemann and Bannister 1986) in estimates of a and b. Vertical heterogeneity in particle concentrations over the depth interval from the surface to $z_{0.1}$ can cause an error in the estimate of b (Weidemann and Bannister 1986). Inspection of transmissometer profiles (e.g., Fig. 2 of Effler et al. 1998) indicates the occurrence of only modest heterogeneity in particle concentration (e.g., <30% difference) (Weidemann and Bannister 1986) within this interval on several occasions over the study period. Overall, errors in the estimates of a and b that are attributable to the uncertainties in the determination of the apparent optical properties are expected to be < 10% and < 15%, respectively, for the vast majority of field conditions encountered.

Spectral average absorption coefficients for PAR for water (a_w, m^{-1}) and for gelbstoff (a_y, m^{-1}) were determined from respective absorption spectra and spectral downwelling irradiance ($E_{d(\lambda)}$) data at $z_{0.1}$ [Eq. (5), Table 1]. The absorption spectrum of water ($a_{w(\lambda)}$) is that reported by Smith and Baker (1981). The spectral average absorption coefficient for particles (a_p) was determined as a residual [Eq. (6), Table 1]. This is less desirable than estimating a_p directly from laboratory measurements (Weidemann and Bannister 1986). However, this approach is supported by the findings of Weidemann and Bannister (1986). They observed good agreement between a and the summation of the independently determined values of a_w, a_y, and a_p in Irondequoit Bay, NY.

Results and Discussion

Interconsistency and Quality Assurance

Several checks were made to establish the interconsistency and veracity of the measurements, and test the assumptions inherent in the calculations. First, depth profiles of R showed the curvilinear (and widely observed) distribution predicted by theory (Kirk 1981a), increasing with depth. Asymptotes were generally reached by $z_{0.1}$, indicative of establishment of the asymptotic radiance distribution, supporting the adopted protocols for sampling and estimation of a and b (Kirk 1981b) and their components (Effler and Perkins 1996a, Weidemann and Bannister 1986).

Semilog plots of the paired measurements of E_d and E_u, and the next day observations of E_o, versus

depth were nearly parallel in subsurface layers, thus the values of K_o, K_d, K_u and K_E (Table 1) were nearly equal. This is expected (Kirk 1994) and has been reported by a number of investigators (Perkins and Effler 1996, Vant and Davies-Colley 1984, Weidemann and Bannister 1986). Additionally, values of $K_{d(PAR)}$ were approximately equal to those determined for K_o (average of 13% difference) and K_d (average of 11% difference), supporting the partitioning of a [see Eq. (5), Table 1] presented subsequently. Undoubtedly, measurements on consecutive days (instead of paired measurements on the same day) contributed to the modest differences observed among the various attenuation coefficients (e.g., see subsequently documented dynamics of K_o).

The estimates of b were quite similar in magnitude to the measurements of T_n, as observed elsewhere (DiToro 1978, Effler 1988, Vant and Davies-Colley 1984, Weidemann and Bannister 1986). The relationship between b and T_n has been described by the following relationship (Effler and Perkins 1996b, Weidemann and Bannister 1986)

$$Tn = \alpha \cdot b \qquad (7)$$

where α is a constant (NTU · m). The value has been observed to fall in the rather narrow range of about 0.8 to 1.25 NTU · m (DiToro 1978, Effler 1988, Effler et al. 1991, Kirk 1981b, Vant and Davies-Colley 1984, Weidemann and Bannister 1986). The average value of α for 31 paired measurements of T_n and estimates of b for Cannonsville Reservoir in 1995 was 1.02 (CV = 0.22), supporting the position that these parameters have essentially equivalent numeric values in this system.

All gelbstoff spectra ($a_{y(\lambda)}$) demonstrated exponential decreases with increasing wavelength, as documented for other lakes and reservoirs (Davies-Colley and Vant 1987, Effler et al. 1991, Kirk 1976, Kirk 1994, Weidemann and Bannister 1986). These spectra have been described by the following relationship (Davies-Colley and Vant 1987)

$$a_{y(\lambda)} = a_{y(440)} \exp [S (440 - \lambda)] \qquad (8)$$

where $a_{y(\lambda)}$ = absorption due to gelbstoff at wavelength λ (400 - 700 nm) (m^{-1}) and S = slope parameter (nm^{-1}). The wavelength of 440 nm has been adopted as the reference wavelength (Davies-Colley and Vant 1987, Kirk 1994). The optical impact of gelbstoff ($a_{y(\lambda)}$) can thus be represented through $a_{y(440)}$, once the value of S is known [Eq. (8)]. The mean value of S for Cannonsville Reservoir was found to be 0.016 nm^{-1}; only modest variations were observed (CV = 0.125). The mean value was well within the relatively narrow range reported for lakes (Davies-Colley and Vant 1987, Effler et al. 1991, Effler and Perkins 1996b) and rivers (Smith et al. 1994).

Spatial Distributions

Longitudinal gradients in attenuating components (Table 2a), and therefore inherent (e.g., Table 2c) and apparent (e.g., Table 2b) optical properties, prevailed along the WBDR axis of the reservoir during the study period of 1995. Example longitudinal profiles are presented here for a conspicuous gradient case (Fig. 2). Conditions near the mouth of the smaller Trout Creek arm of the reservoir (site 3, Fig. 1) were generally similar to those observed at site 4 proximate to the water supply intakes (Table 2, Fig. 2). Concentrations and levels of the attenuating constituents and the magnitudes of the attenuating processes were the greatest, and light penetration the least, in the upstream portions of the reservoir. Reflectance was somewhat higher and $\bar{\mu}$ lower on average at sites 5 and 6 (Table 2b and c), depicting greater contributions of scattering (i.e., particles) relative to absorption at these locations. The spatial structure of the optical properties (Table 2, e.g., Fig. 2) is consistent with the zonation proposed by Effler and Bader (1998) for the reservoir: site 6 as "riverine," site 5 as "transitional," and sites 4, 3, 2, and 1 as "lacustrine." Assuming a boundary midway between sites 4 and 5, the lacustrine portion represents ~ 80% of the total volume when the reservoir is full. The observed spatial structure reflects gradients in: 1) phytoplankton production (Auer 1998) and biomass (Table 2a, e.g., Fig. 2b) in response to nutrient loading (Longabucco and Rafferty 1998) from WBDR, 2) abiotic particle loading from WBDR (Longabucco and Rafferty 1998), 3) particle resuspension that accompanied drawdown in 1995 (Effler et al. 1998), and 4) allochthonous inputs of gelbstoff (Stepczuk et al. 1998).

The features of this general longitudinal structure in optical characteristics were highly dynamic, associated with variations in the processes responsible for the gradient(s). The gradients of September 5 were particularly strong (Fig. 2). For example, $a_{y(440)}$ was about 10 times greater (Fig. 2a) and Chl was about 4 times greater (Fig. 2b) at site 6 compared to site 4; SD was nearly 10 times lower (Fig. 2d), K_x (Fig. 2e) was about 7 times higher, R was nearly twice as great (Fig. 2f), b was more than 10 times greater (Fig. 2g), and a was more than 6 times greater (Fig. 2h) at site 6 than at site 4. Variability was relatively greater in the riverine and transition zones compared to the lacustrine zone during the study (see CV values of Table 2). On average (Table 2), the longitudinal gradients were substantially less than manifested on September 5 (Fig. 2). Values of Chl, T_n, and $a_{y(440)}$ (Table 2a) were about twice as great at site 6 compared to site 4; SD was about 40% lower and K_o nearly 35% higher, on average, at site 6 (Table 2b). Estimated values of b and a were, on

Table 2.–Spatial distributions in optical characteristics in Cannonsville Reservoir, over the April-October interval of 1995.

a. attenuating components

Site	C_T (mg · m^{-3})				T_n (NTU)				$a_{y(440)}$ (m^{-1})			
	$\bar{x}$	n	range	CV	$\bar{x}$	n	range	CV	$\bar{x}$	n	range	CV
1	9.7	27	1.5 - 21.3	0.41	1.9	27	0.6 - 3.6	0.42	0.413	26	0.311 - 0.553	0.16
2	10.3	26	1.7 - 22.1	0.53	2.1	26	0.8 - 4.7	0.48	-	-	-	-
3	11.4	26	1.7 - 33.0	0.64	2.2	26	0.8 - 5.8	0.55	-	-	-	-
4	11.5	27	1.7 - 23.6	0.49	2.5	27	1.0 - 5.6	0.52	0.442	27	0.253 - 0.587	0.16
5	18.9	26	4.2 - 93.1	0.98	4.5	26	1.0 - 19.5	0.98	0.541	6	0.391 - 0.829	0.27
6	22.4	24	2.3 - 106.8	0.95	4.3	22	1.5 - 16.8	0.79	0.875	24	0.426 - 3.984	0.82

b. measured optical characteristics

Site	SD (m)				K_o				R				c_{660}			
	$\bar{x}$	n	range	CV	$\bar{x}$	n	range	CV	$\bar{x}$	n	range	CV	$\bar{x}$	n	range	CV
1	2.7	27	1.6 - 4.7	0.30	0.637	27	0.451 - 0.864	0.15	0.043	8	0.022 - 0.067	0.33	2.308	26	0.477 - 4.013	0.28
2	2.6	25	1.5 - 4.0	0.23	0.643	27	0.386 - 1.194	0.27	0.045	2	0.043 - 0.047	-	2.429	26	0.493 - 3.861	0.27
3	2.4	25	1.3 - 4.2	0.33	0.689	27	0.381 - 1.260	0.30	0.052	2	0.047 - 0.056	-	2.637	24	0.503 - 4.497	0.34
4	2.4	26	1.3 - 4.8	0.38	0.740	27	0.419 - 1.362	0.34	0.045	10	0.027 - 0.056	0.22	2.611	26	0.546 - 4.340	0.34
5	1.8	25	0.6 - 3.0	0.39	0.898	24	0.489 - 2.385	0.47	0.056	9	0.025 - 0.080	0.34	3.265	24	0.765 - 7.696	0.41
6	1.5	22	0.3 - 2.8	0.40	0.984	20	0.574 - 1.934	0.34	0.057	2	0.043 - 0.070	-	3.657	20	0.847 - 5.897	0.31

estimated optical characteristics

Site	$\bar{}$				$\bar{\mu}$				b				a			
	$\bar{x}$	n	range	CV	$\bar{x}$	n	range	CV	$\bar{x}$	n	range	CV	$\bar{x}$	n	range	CV
1	.634	8	0.577 - 0.713	0.07	2.244	8	1.057 - 3.815	0.34	0.438	8	0.365 - 0.534	0.15				
2	.625	2	0.619 - 0.630	0.01	2.658	2	2.070 - 3.246	-	0.501	2	0.413 - 0.589	-				
3	.613	2	0.602 - 0.623	0.02	3.692	2	2.390 - 4.993	-	0.597	2	0.431 - 0.762	-				
4	.627	10	0.598 - 0.668	0.04	2.785	10	1.226 - 4.804	0.36	0.498	10	0.347 - 0.724	0.20				
5	.607	9	0.540 - 0.703	0.09	5.686	9	1.230 - 12.374	0.69	0.809	9	0.387 - 1.472	0.46				
6	.587	2	0.552 - 0.622	0.06	30.564	2	22.64 - 38.48	-	5.406	2	3.023 - 7.788	-				

d. estimated partitioning of a

Site	a_w				a_y				a_p			
	$\bar{x}$	n	range	a_w/a	$\bar{x}$	n	range	a_y/a	$\bar{x}$	n	range	a_p/a
1	0.153	6	0.127 - 0.175	0.346	0.095	6	0.058 - 0.166	0.218	0.200	6	0.082 - 0.302	0.435
4	0.165	7	0.148 - 0.198	0.330	0.084	7	0.039 - 0.129	0.182	0.271	7	0.091 - 0.487	0.488
5	0.173	6	0.157 - 0.190	0.290	0.121	6	0.085 - 0.183	0.209	0.397	6	0.100 - 1.132	0.500

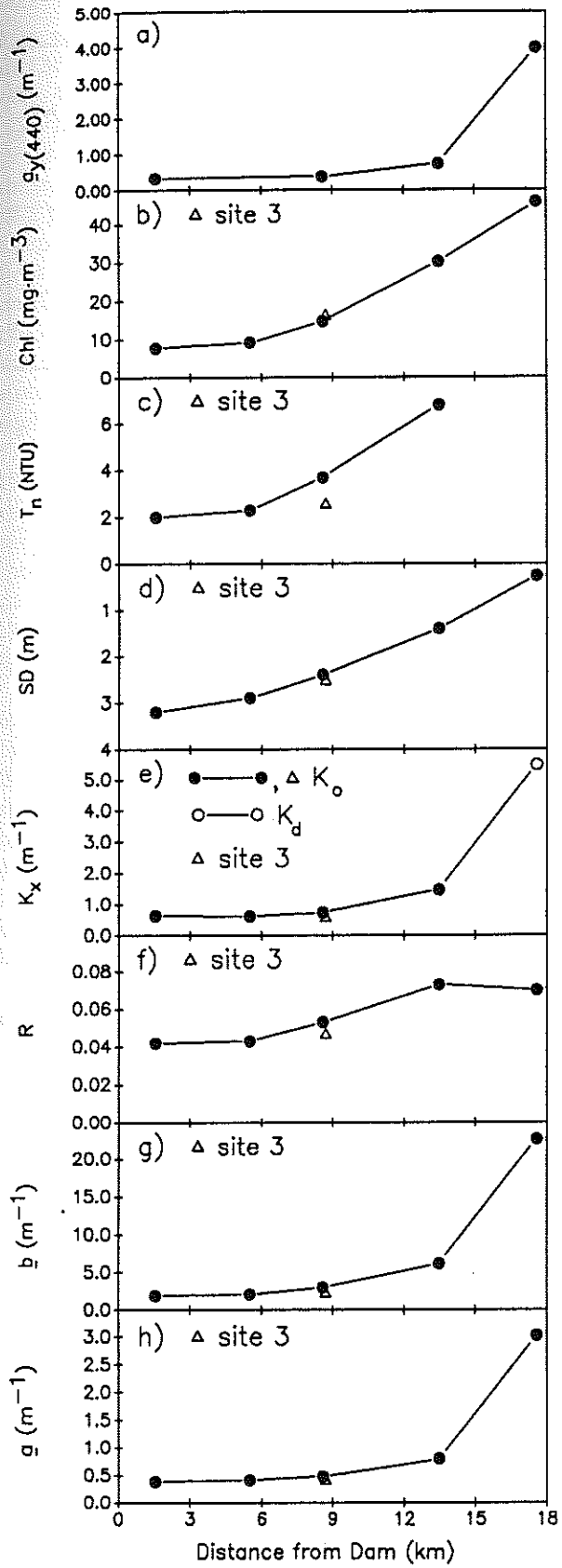

Figure 2.–Longitudinal profiles of optical parameters in Cannonsville Reservoir, September 5, 1995: a) $a_{y(440)}$, b) Chl, c) T_n, d) SD, e) K_x, f) R, g) *b*, and h) *a*.

average, about 2 and 1.6 times greater, respectively, at site 5 than at site 4 (Table 2c). The value of a_w was rather spatially uniform (Table 2d). Estimated values of a_y and a_p were, on average, about 50% greater at site 5 than at site 4 (Table 2d). Though progressive changes in the means were observed for the various optical measures through the lacustrine zone (see Table 2), only the differences in the means of turbidity between sites 1 and 4 were statistically significant ($p = 0.014$).

Gradients in attenuating constituents along the main axis of the reservoir were also manifested in $K_{d(\lambda)}$ spectra (Fig. 3). Most of the upward shift from site 1 to site 5 on September 19 was attributed to the higher scattering at site 5 (Fig. 3a). Note that the shapes of the spectra were rather similar on this day despite the substantial differences in $K_{d(PAR)}$ (Fig. 3a). This is characteristic of the effect of scattering on spectral quality (Phillips and Kirk 1984). In contrast, spatial differences in phytoplankton appear to have played a more important role in regulating the differences in $K_{d(\lambda)}$ spectra on July 24 (Fig. 3b). The higher $K_{d(\lambda)}$ values at site 5 in the lower portion of the PAR interval on this day depict the selective absorption effects of phytoplankton (Fig. 3b). The highest values of $K_{d(\lambda)}$ in all cases were observed at the blue end of the spectrum (Fig. 3), because of the selective absorption of these wavelengths by the levels of gelbstoff and phytoplankton that prevailed in the reservoir. Increases at the red end of the spectrum were due to the selective absorption

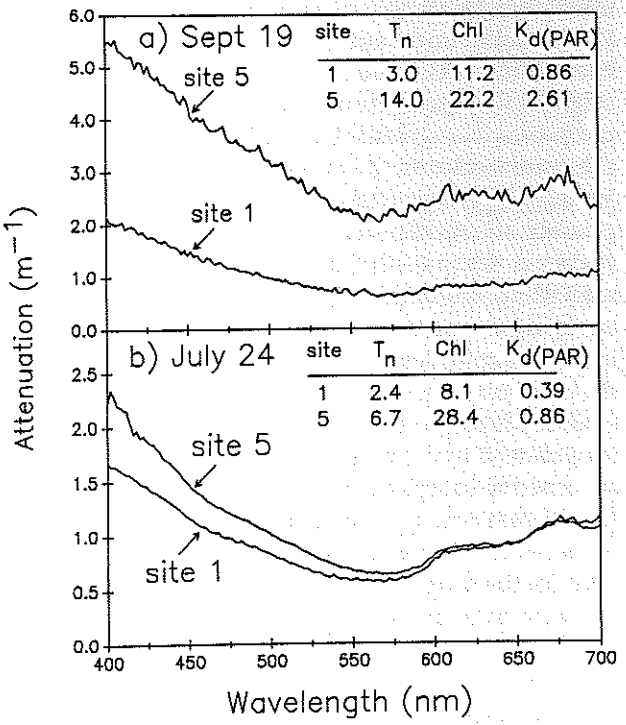

Figure 3.–$K_{d(\lambda)}$ spectra for Cannonsville Reservoir, for selected (2) sites: a) September 19, 1995, and b) July 24, 1995.

properties of water (Smith and Baker 1981) and phytoplankton (Kirk 1994). Modest peaks in $K_{d(\lambda)}$ in the vicinity of the secondary absorption peak of phytoplankton pigments (about 675 nm) (Kirk 1994, Weidemann and Bannister 1986) were apparent. The peak was more conspicuous at site 5 on September 19, consistent with the higher Chl concentrations at that location (Fig. 3a). Minimum attenuation occurred at about 560 nm (Fig. 3).

Temporal Structure

Large temporal variations in attenuating constituents, and therefore inherent and apparent optical properties, occurred in the upper waters of the lacustrine portion of Cannonsville Reservoir over the April-September interval of 1995. The temporal distributions presented here for site 4 (Fig. 4) are generally representative of those found for the other lacustrine sites. Gelbstoff ($a_{y(440)}$) levels varied between 0.35 and 0.6 m^{-1} from April through mid-September (Fig. 4a). These levels fall into the lower portion of the range reported for fresh waters (Davies-Colley and Vant 1987, Kirk 1994). Decreases in $a_{y(440)}$ were observed through May, followed by increases in June, a second minimum in late August and early September, and a decrease to the study minimum in early October (Fig. 4a). Both autochthonous (e.g., primary production) and allochthonous sources are known to contribute to the watercolumn pool of gelbstoff (Bricaud et al. 1981, Davies-Colley and Vant 1987). The lack of correlation between the distributions of $a_{y(440)}$ (Fig. 4a) and Chl (Fig. 4b) indicates primary production is probably not the principal regulator of the distribution of $a_{y(440)}$ in the water column of Cannonsville Reservoir. The average $a_{y(440)}$ reported for the mouth of WBDR (the primary allochthonous source) for the study period (0.68 m^{-1}, CV = 0.44; from Stepczuk et al. 1998) was somewhat greater than the reservoir levels, supporting terrigenous sources as important. However, the disparity in the magnitudes and the temporal distributions in the reservoir (Fig. 4a) and in WBDR (Fig. 2c of Stepczuk et al. 1998) suggest the operation of a loss process(es) for gelbstoff in the reservoir. Gelbstoff is known to be adsorbed to inorganic particles (Kirk 1985). Note that the decreases in $a_{y(440)}$ from mid-summer to early September coincided with increases in inorganic particle PAV in the upper waters (Fig. 4d), supporting adsorption as a potentially important loss process for gelbstoff in the reservoir.

The distribution of Chl at this site in 1995 (Fig. 4b) has been described previously by Effler and Bader (1998). Abrupt changes in Chl concentrations occurred. Peak concentrations ≥ 20 mg · m^{-3} were observed in late

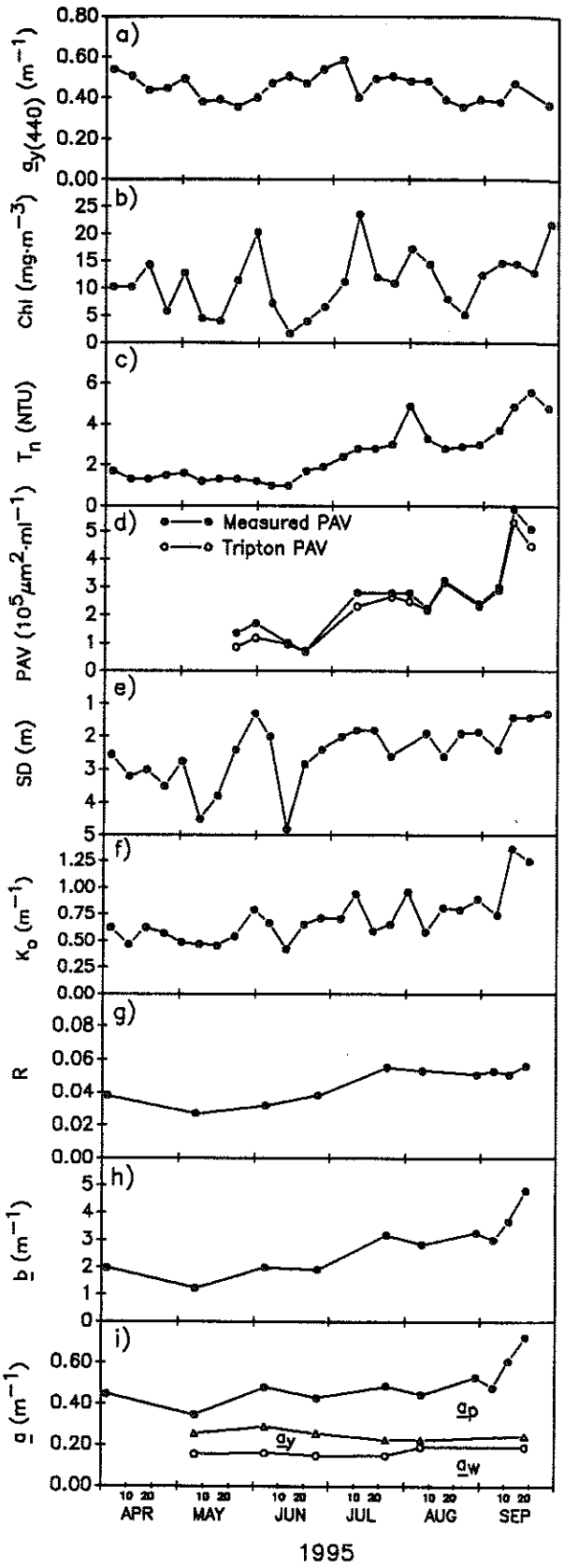

Figure 4.–Dynamics in optical parameters at site 4 in Cannonsville Reservoir in 1995: a) $a_{y(440)}$, b) Chl, c) T_n, d) total PAV and inorganic tripton PAV, e) SD, f) K_o, g) R, h) *b*, and i) *a*.

May, early June, and late September (Fig. 4b). Minima in Chl occurred in May, mid-June, and late August (Fig. 4b). Turbidity remained relatively low (e.g., < 2 NTU) through early June and increased in a largely progressive manner through August. The sharp increase in September is probably attributable to entrainment of a portion of the benthic nepheloid layer with the deepening of the upper mixed layer (Effler et al. 1998). Peak T_n values were observed in early August (>4 NTU) and late September (>5 NTU; Fig. 4c). The distributions of Chl and T_n were not correlated, indicating tripton was important in regulating T_n (particularly in late summer), and other measures of light penetration such as SD (Fig. 4e) and K_o (Fig. 4f). The dynamics of PAV were driven largely by the inorganic tripton fraction (Fig. 4d; R^2 = 0.98). It is estimated this fraction represented about 86%, on average, of the total measured PAV for the study period. The increase in inorganic tripton PAV has been attributed primarily to particles derived from the watershed that have been resuspended largely in response to the drawdown of the reservoir surface (Effler et al. 1998).

Clarity (SD) was highly variable in the reservoir from April through June; thereafter SD was low and more invariant (Fig. 4e; also presented by Effler and Bader 1998). The range of SD observations was 1.3 to 4.8 m. Variations in Chl (Fig. 4b) regulated the dynamics of SD through June [R^2 = 0.8, for 1/SD vs. Chl (Effler and Bader 1998)], a period when T_n remained relatively low (1 to 2 NTU). For example, a conspicuous decrease in SD (Fig. 4e) coincided with the short-lived bloom of late May (Fig. 4b). Clarity was much more insensitive to the substantial changes in phytoplankton biomass observed after June (Fig. 4e). This is consistent with the coupled increases of inorganic tripton PAV (Fig. 4d) and T_n (Fig. 4c), and the established sensitivity of SD to increases in T_n (scattering) in that range (Effler 1988).

The value of K_o varied from 0.42 to 1.35 m^{-1} at this site over the study, corresponding to a range in photic zone depth (assumed at $z_{0.01}$) of about 3.4 to 11 m. On average, $z_{0.01}$ and $z_{0.1}$ were at depths of 6.8 and 3.4 m. The minimum K_o measurement coincided with the minimum Chl observation in June; the maximum value occurred during a T_n peak in September. Inflections in K_o (Fig. 4f) generally tracked those reported for SD (Fig. 4d); e.g., increases in K_o coincided with decreases in SD (and increases in attenuating constituents). However, these two parameters were not precise measures of each other. For example, the product $K_o \cdot$ SD (Effler 1985) was rather variable over the study period at all the monitoring sites; the average CV ranged from 0.17 to 0.21. Thus these two measures of light penetration are not reliable estimators of each other in Cannonsville Reservoir. Variability in the $K_x \cdot$ SD product can often be attributed primarily to variations in the relative contributions of a and b to attenuation (Effler 1985, Effler et al. 1988), as these two optical measurements respond quite differently to the underwater light field (Kirk 1981b, Tyler 1968).

Variations in R (Fig. 4g) reflect changes in the relative contributions of absorption and scattering to attenuation. As R increases, the relative role of scattering (i.e., the ratio b/a) increases (Kirk 1981b). Progressive increases in R occurred over the May-July interval; values remained at the higher level over the August-September period (Fig. 4g). The increases in R are consistent with the influx (e.g., resuspension) of inorganic particles into the water column that occurred over that period (Fig. 4d; also see Effler et al. 1998).

Generally progressive increases in b occurred after early May [Fig. 4h; and as indicated in more temporal detail by T_n (Fig. 4c)], covering a range of about 1 to 5 m^{-1}. The estimated value of a also increased over the same period, but only by a factor of 2; a was estimated to be nearly uniform for the June-August interval, based on the subset of samplings for which measurements of E_d and E_u (i.e., R) were made (Fig. 4i). The distinctly greater response of b relative to a after May is consistent with the introduction of increasing inorganic tripton PAV (Fig. 4d) that absorbs little, relative to the impact on scattering. The light absorption properties of tripton vary substantially. For example, freshly precipitated calcium carbonate scatters light with essentially no absorption (Weidemann et al. 1985), while Kirk (1985) described tripton that rather strongly absorbed light, that was attributed to adsorbed humic substances.

There is indirect evidence that the light absorbed by resuspended tripton in the upper waters of Cannonsville Reservoir in 1995 was small relative to that absorbed by phytoplankton. The dynamics of a were driven largely by variations in a_p (Fig. 4i), and a_p was the largest component of a (Table 2c). The a_p component of a has been partitioned between phytoplankton and tripton particles according to (Effler and Perkins 1996a)

$$a_p = a_p' + K_a \cdot \text{Chl} \qquad (9)$$

where a_p' = spectral average absorption coefficient for tripton (m^{-1}), and K_a = Chl-specific absorption coefficient ($m^2 \cdot$ mg Chl^{-1}). According to linear least squares regression analysis (Fig. 5), variations in Chl explained about 68% of the dynamics observed in a_p (including sites 1, 4, and 5); the best estimates of K_a and a_p' were 0.022 $m^2 \cdot$ mg Chl^{-1} and 0.021 m^{-1}, respectively. This value for K_a is at the upper bound of values included in the critical review of Bannister and Weidemann (1984). The a_p' value should be considered an approximation of the study average; almost certainly temporal variations in this absorping component

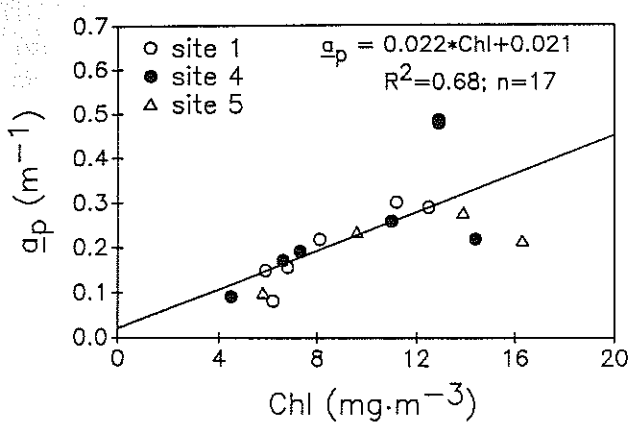

Figure 5.–Evaluation of the dependency of a_p on Chl concentration at site 4 in Cannonsville Reservoir in 1995.

occurred. This estimate serves to establish that absorption by phytoplankton dominated a_p in the reservoir during the study period; e.g., on average a_p' represented only about 10% of a_p at site 4. The modest dynamics in a_w (Fig. 4i) result only from changes in the spectral quality of downwelling irradiance (Weidemann and Bannister 1986) that, in this system, are primarily associated with variations in the concentrations of absorbing particles. Dynamics in a_y (Fig. 4i) also reflect this form of feedback from shifts in spectral quality, but are primarily driven by changes in $a_{y(440)}$.

Partitioning the Components of T_n

The IPA/SAX data (e.g, Fig. 4d, plus size information) can be used to evaluate the role of inorganic tripton in regulating the observed dynamics of T_n (Fig. 4c) and b (Fig. 4h). The light scattering efficiency of inorganic particles larger than about 2.5 µm (area equivalent) diameter converges on a constant value (Kirk 1994); e.g., PAV has a uniform and linear relationship with T_n in this particle size range where diffraction scattering is a good approximation of Mie scattering (Treweek and Morgan 1980). In a study of Skaneateles Lake, NY (Owens et al. 1995), where most of the samples had geometric mean particle diameters > 2.5 µm, a strong relationship (R^2 = 0.94) between paired measurements of T_n and PAV was observed over the T_n range of 1 - 20 NTU (n=140)

$$T_n = (0.48 \cdot PAV) - 0.12 \qquad (10)$$

Inorganic particle assemblages enriched with smaller particles (< 2.5 µm, in diameter) scatter relatively more light (Kirk 1994, cf. Fig. 4.3). Within the context of PAV data, this corresponds to an increase in the proportionality constant (e.g., "slope factor") for the T_n - PAV relationship [e.g., Eq. (10); also see Fig. 7.51a of Effler and Perkins 1996b]. During the course of the drawdown in Cannonsville Reservoir, May through August 1995 (Fig. 6a), the geometric mean particle size ranged from about 2.2 µm to 1.8 µm (Fig. 6b). This enrichment in smaller particle sizes is consistent with the process of sediment resuspension and the progression of drawdown in the reservoir, as smaller particles are known to be preferentially associated with deeper depths in lacustrine systems (e.g., Sly et al. 1982, Thomas et al. 1972). Optically effective PAV values were estimated (Owen 1974), to accommodate the effect of particle size, based on T_n - PAV relationships developed from experiments for different size classes (as reviewed by Effler and Perkins 1996b). These adjustments for enrichment of smaller sizes in the particle assemblage resulted in slope factors greater than the 0.48 value of Eq. (10) (Fig. 7). The adjustments in the "slope factor" were independently checked against Mie theory (see Kirk 1994) calculations (Fig. 7), using the BHMIE algorithm of Bohren and Huffman (1983) to estimate the average scattering coefficient between 86 and 94 degrees, integrating over the experimental size distribution, and assuming a refractive index of 1.17 (relative to the water) for the particles [typical value for inorganic particles (Kirk 1994)]. The relative scattering coefficients were normalized to the unaltered sample size distribution for comparison (Fig. 7). While experiments for "large particle enrichment" were not conducted, the computations of

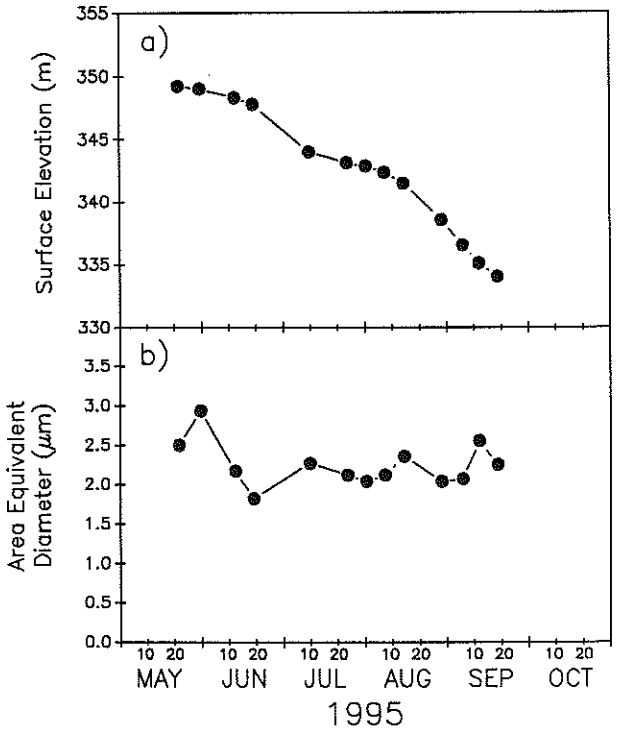

Figure 6.–Dynamics of geometric mean particle size in the upper waters at site 4 in Cannonsville Reservoir in 1995.

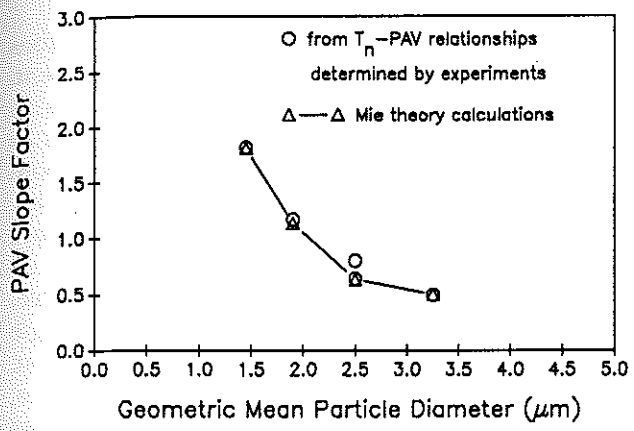

Figure 7.–PAV "slope factor" as a function of median particle diameter, obtained in two ways, from T_n - PAV relationships determined by experiments and Mie theory calculations.

Kirk (1994, Fig. 4.3) show that a relatively constant scattering coefficient would result for geometric mean particle sizes greater than about 2.5 μm. This is supported by the high degree of linearity observed between T_n and PAV in the Skaneateles Lake study (Owens et al. 1995).

The temporal distribution of inorganic tripton turbidity ($T_{n/t}$), predicted from the corresponding effective (i.e., size adjusted) PAV values, is compared here to the distribution of measurements of T_n, for the subset (n = 13) of observations for which IPA was conducted (Fig. 8). The error bars on the predicted $T_{n/t}$ values (Fig. 8) represent 50% of the turbidity increment which would be associated with adding the "organic" and "diatom" PAV. This level of uncertainty in the predictions is not considered limiting to the analysis, as it is relatively minor compared to the observed seasonality in T_n and the predicted trend in $T_{n/t}$ (Fig. 8). This analysis establishes the dominant role of inorganic tripton, and the process of sediment

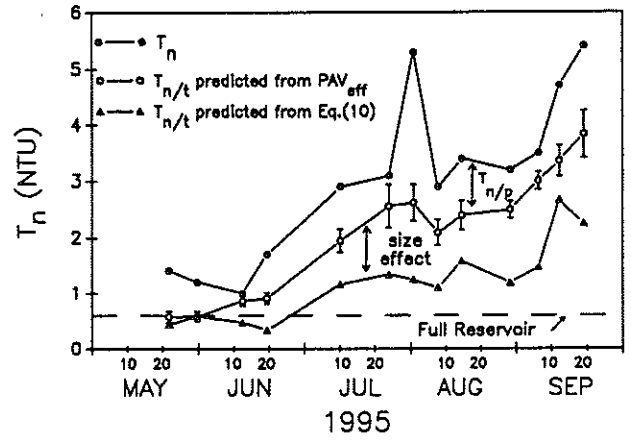

Figure 8.–Comparison of temporal distributions of T_n observations and estimates of $T_{n/t}$ at site 4 in Cannonsville Reservoir in 1995.

resuspension, in regulating the increases in T_n (and b) observed in Cannonsville Reservoir in 1995, and thereby couples this feature of water quality to the reservoir's operation (drawdown) (Effler et al. 1998). According to linear least squares regression, the predicted changes in $T_{n/t}$ explain 85% of the observed variations in T_n. On average (n=13), $T_{n/t}$ represented 68% of T_n for the study period. Predictions of $T_{n/t}$ for the case of no size adjustments to PAV (i.e., for scenario of area equivalent diameter > 2.7 μm) are also presented (Fig. 8) to demonstrate the important influence of the shift to smaller particle sizes in regulating the observed increases in T_n.

The residual, T_n minus $T_{n/t}$, is attributed to phytoplankton ($T_{n/p}$; i.e., contribution of detritus assumed negligible). The partitioning of scattering according to the contributions of phytoplankton and inorganic tripton can be described according to (e.g., Effler and Perkins 1996a, Weidemann and Bannister 1986)

$$b = K_b \cdot \mathrm{Chl} + b' \qquad (11)$$

where b' = spectral average scattering coefficient for inorganic tripton (m^{-1}), and K_b = Chl-specific scattering coefficient ($m^2 \cdot mg\ Chl^{-1}$). The values of K_b determined from the residual estimates of $T_{n/P}$ support the veracity of the partitioning of T_n components presented (Fig. 8), as they are generally consistent with values reported in the literature (Effler and Perkins 1996a, Weidemann and Bannister 1986). The mean value of K_b was 0.076 $m^2 \cdot mg\ Chl^{-1}$ (median K_b = 0.064, CV = 0.55). Eight (of 13) values of K_b fell in the range of 0.05 to 0.15 $m^2 \cdot mg\ Chl^{-1}$ (10 values in the range of 0.04 to 0.13 $m^2 \cdot mg\ Chl^{-1}$), a range that brackets the observations of Weidemann and Bannister (1986) for Irondequoit Bay and 60% of the observations reported for Onondaga Lake (Effler and Perkins 1996a). The relatively wide variations in the estimates of K_b are not unexpected, as values of K_b are known to vary widely as a function of the composition of the phytoplankton assemblage (Bricaud et al. 1983, Weidemann and Bannister 1986). Errors in the underlying measurements and inherent to the residual calculation protocol adopted also undoubtedly contributed to the variability in the estimates of K_b.

Evaluation of Scenarios

Expressions have been developed that quantitatively accommodate the contributions of a and b in regulating the commonly used measures of light penetration, K_d and SD. These relationships, or models, can be used to predict values of K_d and SD for scenarios of systematic changes in attenuating constituents. Kirk

(1981a) developed the following expression for K_d, based on Monte-Carlo analyses of the underwater light field

$$K_d = (a^2 + 0.256ab)^{0.5} \quad (12)$$

Based on contrast transmittance theory, it has been demonstrated that SD is inversely proportional to the sum of K_d and c (Preisendorfer 1986, Tyler 1968), as described by

$$SD = \Gamma \cdot (K_d + c)^{-1} \quad (13)$$

where Γ = constant (dimensionless). Priesendorfer (1986) describes it as a "quasi-constant," as it has been demonstrated to vary somewhat in response to uncontrolled conditions (e.g., wave action, cloud cover) that prevail during field measurements. The typical range of Γ is 8.0 to 9.6 (Preisendorfer 1986). Application of the contrast transmittance theory to the 1995 Cannonsville Reservoir data base (Fig. 9; subset of data for which a and b estimates are available) yields a single best estimate of Γ = 8.2. The modest scatter observed in the relationship (Fig. 9) is attributable to variations in the environmental conditions under which measurements were made and imperfections in the measurements themselves (Effler and Perkins 1996a). This system-specific relationship (Fig. 9) represents a mechanistically sound (Preisendorfer 1986, Tyler 1968) and reliable (e.g., R^2 = 0.81) basis to project the implications of changes in a and b, mediated by changes in the concentrations of attenuating substances, on the clarity of this reservoir.

Scenarios for the two major attenuating constituents, phytoplankton and inorganic tripton, are evaluated here, as both may be subject to management-based reductions. Gelbstoff scenarios are not included here because this constituent is not presently a substantial component (e.g., predictions of

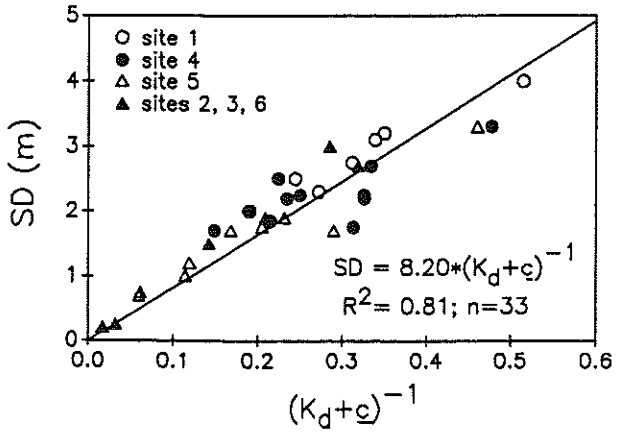

Figure 9.–Application of the contrast transmittance theory for SD at site 4 in Cannonsville Reservoir. Slope is equal to N [Eq. (13)].

K_d and SD are relatively insensitive to realistic variations in a_y), nor is clear that it is subject to management. Three scenarios are evaluated: 1) reductions in phytoplankton biomass (case 2), 2) reductions in inorganic tripton (case 3), and 3) reductions in both phytoplankton biomass and inorganic tripton (Case 4). The simulations of K_d and SD [Γ=8.2; Eq. (13)] are made for site 4 conditions, for the subset of 13 days on which IPA characterizations (Fig. 8) were available. Average values of a_w and a_y (Table 2), and the single best estimates of K_a and a_p^*, are invoked throughout. The individual values of K_b, estimated by difference, are retained, and values of $b' = T_{n/t}$ are invoked for case 2. The scenarios of reductions in phytoplankton biomass invoke a temporal distribution of 0.5 x Chl. Reductions in external phosphorus loading necessary to reduce the summer average Chl concentration of the epilimnion by various increments can be evaluated with the nutrient-phytoplankton model for the reservoir (Doerr et al. 1998). The reductions in inorganic tripton scenarios invoke $b' = 0.6\ m^{-1}$, equivalent to the estimates of $T_{n/t}$ in May (Fig. 8) before significant drawdown commenced. This scenario addresses the issue of the relative impact of drawdown on these measures of light penetration. However, it should be considered only semi-quantitative at this time, as the extent to which the value of $T_{n/t}$ = 0.6 NTU applies for the entire stratification interval of a year in which the reservoir remains full is not yet established. Further, there is probably an interplay between reservoir operation and Chl (Owens et al. 1998a). The "base" case (case 1; basis of evaluation of the impact of the scenarios) corresponds to the existing conditions predicted with the invoked and assumed values for the attenuating components.

Comparisons of the scenarios to the base case are presented graphically (Fig. 10) and as predicted averages (Table 3). The base case predictions differ somewhat from observations because of the assumptions and invoked conditions adopted for all the simulations, as well as imperfections in the measurements. However, these differences are modest; e.g., the predicted mean K_d and SD values for the base case were within 7% and 2%, respectively, of the observations (Table 3). Noteworthy increases in light penetration, as measured by these two parameters, are predicted for all three scenarios (Fig. 10, Table 3). Further, the differences in the predicted responses of these two parameters are instructive with respect to the sensitivity of each to different attenuating constituents. The value of K_d is more sensitive to incremental changes in absorbing components; SD is more sensitive to changes in scattering constituents [Eqs. (13) and (14)]. For example, a 23% decrease in average K_d and an 18% increase in average SD (relative to base case; Table 3) are predicted for the reduction in phytoplankton

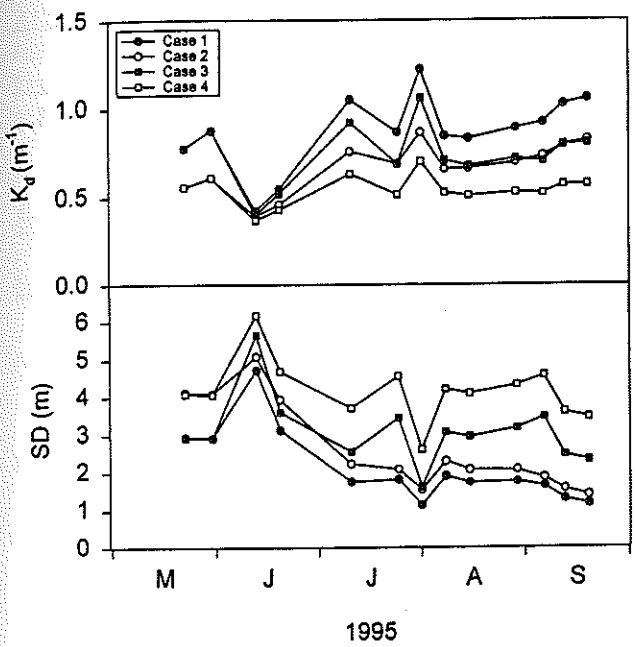

Figure 10.–Predicted temporal distributions of measures of light penetration at site 4 in Cannonsville Reservoir for four cases (including three scenarios of reductions in attenuating constituents; see Table 3): (a) K_d, and (b) SD.

biomass (absorbs and scatters) scenario (case 2), while the decrease in K_d is only 15% compared to a 40% increase in SD for the reduced tripton (scatters, with only minor absorption; case 3, Table 3). A decrease of 38% in average K_d and an increase of 91% in average SD are predicted for the scenario of combined reductions of Chl and inorganic tripton (case 4, Table 3). The predicted temporal distributions of the tripton reduction scenarios increasingly diverge from the base case through the simulation interval (Fig. 10a and b), consistent with the progressive increase in $T_{n/t}$ (Fig. 8). Note that nearly equal values of K_d are predicted for cases 2 and 3 for the last month and a half (Fig. 10a) when $T_{n/t}$ was high (in 1995), an interval for which substantially higher SD values are predicted for case 3.

Partitioning K_d for Phytoplankton Modeling

The partitioning of light attenuation between phytoplankton and non-phytoplankton components has often been described according to (e.g., Bannister 1974, Field and Effler 1983, Megard et al. 1979)

$$K_d = k_c \cdot Chl + k_w \qquad (14)$$

where k_c = Chl-specific spectral average attenuation coefficient for phytoplankton ($m^2 \cdot mg^{-1}$ Chl), and k_w = the spectral average attenuation coefficient for all non-phytoplankton components (m^{-1}). It is necessary to quantify this partitioning [e.g., Eq. (14)] in mechanistic nutrient-phytoplankton models, to specify the availability of penetrating light to support production and to accommodate the feedback from changes in phytoplankton biomass (the "self-shading" effect, e.g., Chapra 1997). Operationally, the coefficient values for the partitioning have usually been determined by linear regression; the values of k_c and k_w correspond to the slope and y-intercept, respectively, resulting from the regression of K_d on Chl (e.g., Megard et al. 1979). However, this method of estimation is inappropriate for Cannonsville Reservoir in 1995, because of the systematic temporal trend in $T_{n/t}$ (Fig. 8; an important component of k_w) that was uncoupled from the dynamics of Chl (Fig. 4b and c).

An alternate approach has been adopted here to specify the coefficients k_c and k_w for site 4 in Cannonsville Reservoir, that is appropriate for the dynamics observed in 1995 and is expected to have general utility for the lacustrine zone of the reservoir for other years. The value of k_w was independently calculated [Eq. (12)] from the non-phytoplankton components, a_w, a_y, a_p', and b', for the subset of data for which $T_{n/t}$ estimates are available (e.g., Fig. 8; n = 13). The sum of the absorbing components was kept constant at the same average value adopted in the evaluation of scenarios (Fig. 10), and b' varied according to the estimates of $T_{n/t}$ (Fig. 8). The calculations were generally insensitive to the modest changes in the non-phytoplankton absorbing components encountered in the program (e.g., Table 2). The calculated value of k_w increased from less than 0.35 m^{-1} in May to nearly 0.6 m^{-1} in September (Fig. 11a), consistent with the calculated increase in $T_{n/t}$ (b'; Fig. 8). A rather strong (R^2 = 0.87) empirical negative relationship between k_w and reservoir elevation emerges (Fig. 11b), consistent with the findings of Effler et al. 1998, that resuspension of inorganic particles in the reservoir in 1995 was largely driven by drawdown. The three observations from the fall mixing period were eliminated from the analysis, as there is evidence that entrainment of the benthic nepheloid layer (e.g., a potential input to $T_{t/n}$ that is not directly related to drawdown) contributed to $T_{n/t}$ levels during that interval (Effler et al. 1998). The incorporation of the K_w - elevation relationship (Fig. 11b) into the nutrient-phytoplankton model for the reservoir (Doerr et al. 1998a) supports the independent specification of k_w from the model's hydrologic submodel (also see Owens et al. 1998). The value of k_c was estimated as the slope from the linear least squares regression of $k_c \cdot$ Chl (calculated as the difference, K_d minus k_w) on Chl (y-intercept = 0, specified; Fig. 11c), based on the same data subset. We attribute the scatter in this relationship to errors inherent in such residual calculations, species-specific differences of the phytoplankton, and measure-

Table 3.–Observed and predicted average K_d and SD values for selected scenarios.

Case	$\overline{K_d}$ (m^{-1})	$\overline{SD}$ (m)	Comments
observed	0.81	2.3	observations for subset of IPA (n = 13)
No. 1	0.87	2.2	base case
No. 2	0.67	2.6	Chl = 0.5 x $Chl_{observed}$, observed b'
No. 3	0.74	3.1	b' = 0.6 m^{-1}, observed Chl
No. 4	0.54	4.2	Chl = 0.5 x $Chl_{observed}$, b' = 0.6 m^{-1}

ment errors. The best estimate of k_c (0.021 $m^2 \cdot mg^{-1}$ Chl) is in the range of values reported for other systems (Field and Effler 1983, Megard et al. 1979), and has been adopted by Doerr et al. (1998a).

Management Perspectives

Cannonsville Reservoir is an optically complex system, as strong longitudinal gradients and uncoupled temporal variations in attenuating constituents occur. The optical regime of the reservoir is apparently mostly controlled by phytoplankton biomass when it is full. Inorganic tripton becomes the regulating constituent of turbidity, and other measures of light penetration, as the impoundment is drawn down, thereby linking these aspects of water quality to operation of the reservoir. An earlier manuscript in this issue of the journal (Effler et al. 1998) established that the influx of tripton to the water column was largely attributable to the sediment resuspension process, and that the origin of these inorganic particles was the watershed. Predictions with optics models demonstrated substantial improvements in light penetration could be achieved through systematic reductions in phytoplankton biomass (e.g., reduction of external nutrient loading) and/or inorganic tripton (e.g., erosion control). However, the benefits of reductions in phytoplankton biomass with respect to turbidity and measures of light penetration would be masked in major drawdown years as a result of resuspension of tripton. Erosion control in the watershed may also be a viable management approach to protect the optical esthetics of the reservoir, but the extent and character of the linkage between external loads of tripton and watercolumn concentrations should first be established. Additionally, light attenuation has been partitioned between the phytoplankton and non-phytoplankton components in this manuscript, and an expression to predict the non-phytoplankton component as a function of elevation (drawdown) has been developed to support quantification of light availability in the nutrient-phytoplankton model for the reservoir (subsequently in this issue; Doerr et al. 1998a).

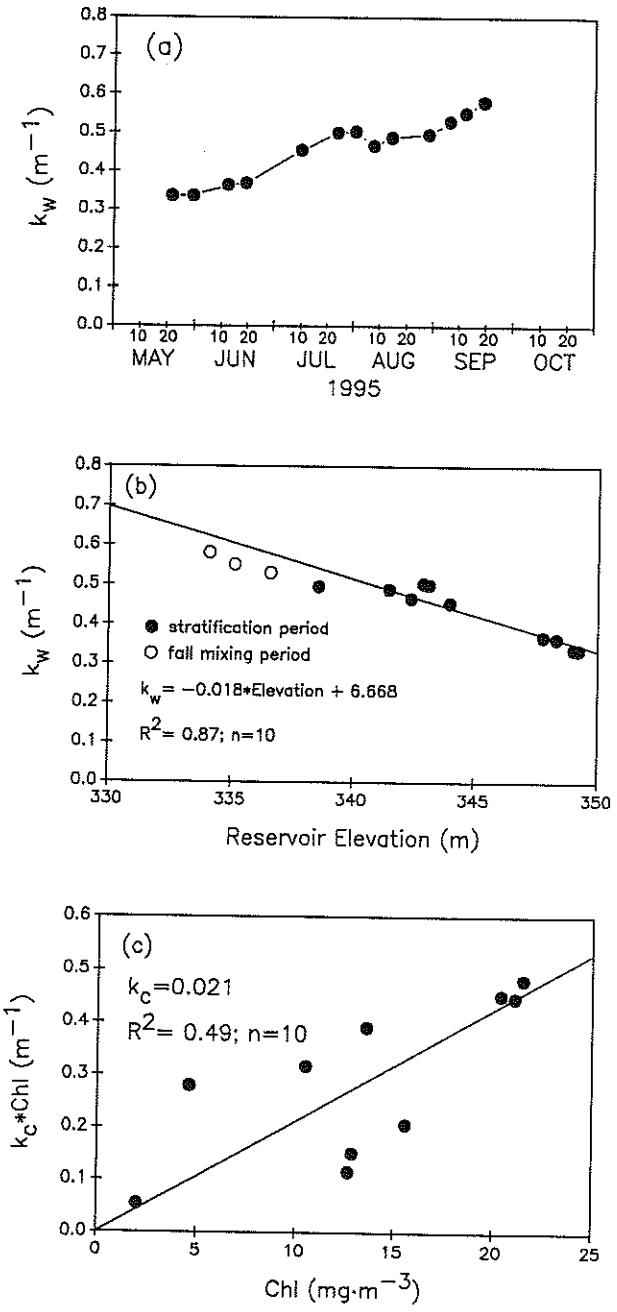

Figure 11.–Relationships for k_w and estimation of k_c [Eq. (14)] at site 4 in Cannonsville Reservoir: (a) k_w as a function of time, (b) k_w as a function of reservoir elevation, and (c) determination of k_c.

ACKNOWLEDGMENTS: This study was supported by the New York City Department of Environmental Protection. This manuscript benefited from the critical review of D. Smith.

References

American Public Health Association. 1992. Standard methods for the examination of water and wastewater, 18th ed. American Public Health Association, Washington, DC.

Auer, M. T. and B. E. Forrer. 1998. Development and parameterization of a kinetic framework for modeling light- and phosphorus-limited phytoplankton growth in Cannonsville Reservoir. Lake and Reserv. Manage. 14(2-3):290-300.

Bannister, T. T. 1974. Production equations in terms of chlorophyll concentration, quantum yield, and upper limit to production. Limnol. Oceanogr. 19:1-12.

Bannister, T. T. and A. D. Weidemann. 1984. The maximum quantum yield of phytoplankton photosynthesis in situ. J. Plankton Res. 6:275-292.

Bohren, C. F. and D. R. Huffman. 1983. Absorption and scattering of light by small particles. John Wiley & Sons, NY.

Bricaud, A., A. Morel and L. Prieur. 1983. Optical efficiency factors of some phytoplankters. Limnol. Oceanogr. 28:816-832.

Chapra, S. C. 1997. Surface water-quality modeling. McGraw-Hill, NY.

Cooke, G. D., E. B. Welch, S. A. Peterson and P. R. Newroth. 1993. Restoration and management of lakes and reservoirs, 2nd ed. Lewis, Ann Arbor, MI.

Davies-Colley, R. J. and W. N. Vant. 1987. Absorption of light by yellow substances in freshwater lakes. Limnol. Oceanogr. 323:416-425.

DiToro, D. M. 1978. Optics of turbid estaurine waters: approximations and applications. Wat. Res. 12:1059-1068.

Doerr, S. M., E. M. Owens, R. K. Gelda, M. T. Auer and S. W. Effler. 1998a. Development and testing of a nutrient-phytoplankton model for Cannonsville Reservoir. Lake and Reserv. Manage. 14(2-3):301-321.

Effler, S. W. 1985. Attenuation versus transparency. J. Environ. Engr. Div. ASCE 111:448-459.

Effler, S. W. 1988. Secchi disc transparency and turbidity. J. Environ. Eng. 144:1436-1447.

Effler, S. W. and A. Bader. 1998. A limnological analysis of Cannonsville Reservoir, NY. Lake and Reserv. Manage. 14(2-3):125-139.

Effler, S. W., and C. M. Brooks. 1998. Gradients and dynamics in downward flux and settling velocity in Cannonsville Reservoir. Lake and Reserv. Manage. 14(2-3):213-224.

Effler, S. W., R. K. Gelda, D. L. Johnson and E. M. Owens. 1998. Sediment resuspension in Cannonsville Reservoir. Lake and Reserv. Manage. 14(2-3):225-237.

Effler, S. W. and M. G. Perkins. 1996a. An optics model for Onondaga Lake, Lake and Reserv. Manage. 12:115-125.

Effler, S. W. and M. G. Perkins. 1996b. Optics (Chapter 7). *In:* S. W. Effler (ed.). Limnological and engineering analysis of a polluted urban lake. Prelude to the environmental management of Onondaga Lake, New York. Springer-Verlag, NY.

Effler, S. W., M. G. Perkins and D. L. Johnson. 1991. Optical heterogeneity in Lake Champlain. J. Great Lakes Res. 17:322-332.

Field, S. D. and S. W. Effler. 1983. Light attenuation in Onondaga Lake, NY, USA, 1978. Arch. Hydrobiol. 98:409-421.

Jerome, J. H., R. P. Bukata and J. E. Burton. 1983. Spectral attenuation and irradiance in the Laurentian Great Lakes. J. Great Lakes Res. 9:60-68.

Johnson, D. L., J. F. Jiao, S. G. DosSontos and S. W. Effler. 1991. Individual particle analysis of suspended materials in Onondaga Lake. Environ. Sci. Technol. 25:736-744.

Kirk, J. T. O. 1976. Yellow substance (gelbstoff) and its contribution to the attenuation of photosynthetically active radiation in some inland and coastal southeastern Australian waters. Aust. J. Mar. Freshwat. Res. 27:61-71.

Kirk, J. T. O. 1981a. A Monte-Carlo study of the nature of the underwater light field in, and the relationship between optical properties of, turbid yellow waters. Aust. J. Mar. Freshwat. Res. 32:517-532.

Kirk, J. T. O. 1981b. Estimation of the scattering coefficients of natural waters using underwater irradiance measurements. Aust. J. Mar. Freshwat. Res. 533-539.

Kirk, J. T. O. 1985. Effects of suspensoids (turbidity) on penetration of solar radiation in aquatic ecosystems. Hydrobiol. 125:194-208.

Kirk. J. T. O. 1994. Light and photosynthesis in aquatic ecosystems. 2nd edition. Cambridge University Press, Cambridge.

LI-COR. 1982. Radiation measurement. LI-COR Corp. Lincoln, NB. 42 p.

Longabucco, P. and M. Rafferty. 1998. Analyis of material loading to Cannonsville Reservoir: advantages of event-based sampling. Lake and Reserv. Manage. 14(2-3):197-212.

Megard, R. O., W. S. Combs, P. D. Smith and A. S. Knoll. 1979. Attenuation of light and daily integral rates of photosynthesis attained by planktonic algae. Limnol. Oceanogr. 24:1038-1050.

Owen, R. W. 1974. Optically effective area of particle ensembles in the sea. Limnol. Oceanogr. 19:584-590.

Owens, E. M., S. W. Effler, S. M. Doerr, R. Gelda, E. Schneiderman, D. G. Lounsbury and C. L. Stepchuk. 1998a. A strategy for reservoir model forecasting based on historic meteorological conditions. Lake and Reserv. Manage. 14(2-3):322-331.

Owens, E. M., R. K. Gelda, S. W. Effler and J. M. Hassett. 1998b. Hydrologic analysis and model development for Cannonsville Reservoir. Lake and Reserv. Manage. 14(2-3):140-151.

Owens, E. M., D. L. Johnson, S. W. Effler and M. G. Perkins. 1995. Phase 2: Skaneateles Lake Hydrodynamic/Turbidity Investigation. Submitted to the City of Syracuse, Syracuse, NY.

Parsons, T. R., J. Marta and C. M. Lalli. 1984. Chemical and biological methods for seawater analysis. Pergamon Press New York, NY.

Perkins, M. G. and S. W. Effler. 1996. Optical characteristics of Onondaga Lake; 1968-1990. Lake and Reserv. Manage. 12:103-113.

Phillips, D. M. and J. T. O. Kirk. 1984. Study of the spectral variation of absorption and scattering in some Australian coastal waters. Aust. J. Mar. Freshwat. Res. 35:635-644.

Preisendorfer, R. W. 1986. Secchi disc science: Visual optics of natural waters. Limnol. Oceanogr. 31:909-926.

Sly, P. G., R. L. Thomas and B. R. Pelletier. 1982. Comparison of sediment energy-texture relationships in marine and lacustrine environments. Hydrobiol. 91:71-84.

Smith, D. G. and R. Maasdam. 1994. New Zealand national river water quality network, 1. Design and physico-chemical characterization. New Zea. J. Mar. and Freshwat. Res. 28:19-35.

Smith, R. C. and K. S. Baker. 1981. Optical properties of the clearest natural waters (200-800 nm). Appl. Opt. 20:177-184.

Stepczuk, C., A. Martin, P. Longabucco, J. A. Bloomfield and S. W. Effler. 1998. Allochthonous contributions of THM precursors in a eutrophic reservoir. Lake and Reserv. Manage. 14(2-3):344-355.

Thomas, R. L., A. L. W. Kemp and C. F. M. Lewis. 1972. Distribution, composition and characteristics of the surface sediments of Lake Ontario. J. Sediment Petrol. 42:66-84.

Treweek, G. P. and J. J. Morgan. 1980. Prediction of suspension turbidities from aggregate size distribution. *In:* M.C. Kavanaugh and J.O. Leckic (eds.). Particulates in water, advances in chemistry series, No. 189, American Chemical Society, Washington, DC.

Tyler, J. E. 1968. The Secchi disc. Limnol. Oceanogr. 13:1-6.

Vant, W. N. and R. J. Davies-Colley. 1984. Factors affecting clarity of New Zealand lakes. New Zealand J. Marine Freshwat. Res. 18:367-377.

Weidemann A. D. and T. T. Bannister. 1986. Absorption and scattering coefficients in Irondequoit Bay. Limnol. Oceanogr. 31:567-583.

Weidemann, A. D., T. T. Bannister, S. W. Effler and D. L. Johnson. 1985. Particle and optical properties during $CaCO_3$ precipitation in Otisco Lake. Limnol. Oceanogr. 30:1078-1083.

Yin, C. Q. and D. L. Johnson. 1984. Sedimentation and particle class balances in Onondaga Lake, NY. Limnol. Oceanogr. 29:1193-1201.